

Networked Acoustic Modems for Real-Time Data Telemetry from Distributed Subsurface Instruments in the Coastal Ocean: Application to Array of Bottom-Mounted ADCPs

DANIEL L. CODIGA

Graduate School of Oceanography, University of Rhode Island, Narragansett, Rhode Island

JOSEPH A. RICE

Department of Physics, Naval Postgraduate School, Monterey, California

PAUL A. BAXLEY

Acoustics Branch, Space and Naval Warfare Systems Center, San Diego, California

DAVID HEBERT

Graduate School of Oceanography, University of Rhode Island, Narragansett, Rhode Island

(Manuscript received 5 May 2004, in final form 4 October 2004)

ABSTRACT

Through the winter and spring of 2002, networked acoustic modems demonstrated real-time wireless data telemetry from an array of bottom-mounted acoustic Doppler current profilers (ADCPs) on the inner continental shelf 20–60 m deep off of Montauk Point, New York. To achieve typical temporal and spatial sampling needs for data assimilative numerical modeling, the array spanned 10 km \times 10 km and transmitted data each \sim 2 h. Network nodes included five sensors, each an ADCP with acoustic modem housed in a trawl-resistant bottom frame; five repeaters that are individual acoustic modems on near-bottom taut-wire moorings; and two gateways, each a buoy with a subsurface acoustic modem and topside cellular modem allowing for two-way communication with the shore. Deliveries from an ADCP adjacent to the gateway buoy were more than 97% successful through both winter and spring. Deliveries from ADCPs 5 km from the gateway averaged 25% (86%) reliability in winter (spring). Winter performance degrades because of upward-refracting sound speed profiles that limit direct acoustic paths, and strong winds that disrupt sea surface reflectivity and increase ambient noise. Reliability improved up to 36% due to the receive-all gateway mode, and more than doubled for certain node pairs due to a handshake protocol incorporating an automatic repeat request. Shore-based network control demonstrated adaptive sampling by changing ADCP vertical and temporal resolution, and network data path rerouting in response to unplanned events, such as trawling impacts. Networked acoustic modems are well suited for coastal ocean-observing systems, particularly at sites such as this where seafloor cables and surface buoys are vulnerable to fishing and shipping activities.

1. Introduction

This article presents results of a several month coastal ocean deployment of networked acoustic modems. The network provided a subsurface wireless

communication system, akin to that envisioned in Curtin et al. (1993), for real-time telemetry of data from an array of deployable, autonomous oceanographic sensors that are distributed across a region of the continental shelf. These results build on the initial system development and preliminary modem performance tests reported by Codiga et al. (2004). Here, the moored array spans a 10 km \times 10 km region of the coastal ocean off the northeast coast of North America near Montauk Point, New York, and Block Island, Rhode

Corresponding author address: Dr. Daniel L. Codiga, Graduate School of Oceanography, University of Rhode Island, Narragansett, RI 02882-1197.
E-mail: d.codiga@gso.uri.edu

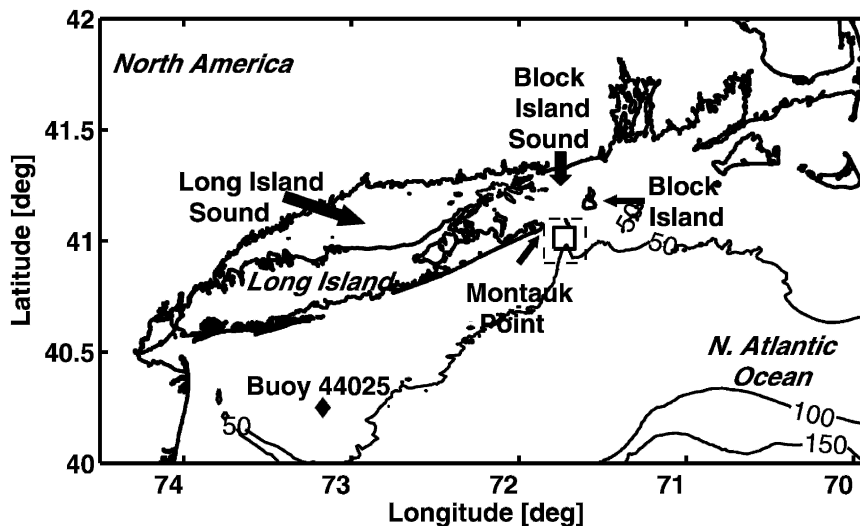


FIG. 1. View of region including 50-, 100-, and 150-m isobaths: buoy 44025 (diamond), the source of wind data; the experiment site (solid box), expanded in Fig. 3; and the area from which historical CTD casts used in Fig. 5 are taken (dashed box).

Island (Fig. 1). The area is subject to heavy trawl fishing and commercial shipping traffic. These hazards create a challenge for real-time data telemetry because they make cabling infeasible and the maintenance of multiple surface buoys impractical. The alternative approach that is demonstrated here consists of a network of acoustic modems that enables subsurface delivery of data from numerous oceanographic sensors to one or two surface buoys that are in communication with the shore.

Typically, a primary use for the real-time data streams generated by coastal ocean observation systems is to facilitate data assimilative numerical modeling of circulation and water properties. To this end, goals for real-time sampling commonly include 1) data acquisition at least several times daily for durations of several weeks to months, so that tides are resolved and subtidal fluctuations can be isolated; and 2) instrument deployment in an array at least 10 km across to capture the spatial structure on scales of at least several kilometers. The present results are from a system that achieves these aims.

Elements of an undersea acoustic network include sensor nodes, repeater nodes, and gateway nodes, as motivated and explained in Codiga et al. (2004). Sensor nodes are oceanographic instruments that are physically connected to acoustic modems. The sensors that are the focus of this study are a set of five upward-looking acoustic Doppler current profilers (ADCPs; Gordon 1996), each deployed in a trawl-resistant bottom frame that enables azimuthally omnidirectional acoustic modem signaling that is required by the net-

work. A moored video plankton recorder (VPR; e.g., Davis et al. 1996), deployed as part of the array to characterize zooplankton distributions, was also equipped with an acoustic modem and participated as a sensor node in the network. Repeater nodes are individual acoustic modems within a few meters of the seafloor, configured as short in-line subsurface moorings (see Fig. 3 of Codiga et al. 2004) that are not protected against trawling gear. Their purpose is to provide connectivity between sensor nodes via concatenation of shorter acoustic links, thus permitting wider area coverage by the available suite of sensor nodes. The deployment of repeaters with no trawl protection was justified by their low replacement cost relative to source nodes, by budgetary constraints that limited the number of trawl-resistant bottom frames, and by the network capability for flexible real-time rerouting of data pathways in response to loss of an individual node due to trawling. Gateway nodes provide communication between the subsurface network and the user or some terrestrial network infrastructure. In this experiment gateways are buoys at the air-sea interface, incorporating both a subsurface acoustic modem and a topside cellular digital packet data (CDPD) modem for a radio connection to the shore via the cellular telephone grid.

2. Instruments and methods

We report on the fourth main field deployment in the Front-Resolving Observation Network with Telemetry (FRONT) project. FRONT4 had two main phases: the winter of 2002 (WI02; from January to early March),

followed by the spring of 2002 (SP02; from mid-March to June).

a. Acoustic modems

The acoustic modems are Benthos (formerly Data-sonics) model 885 series, operating at 9–14 kHz, with a source level of 180 dB relative to 1 μ Pa at 1 m, a net information rate of 300 bits per second (bps), and Hadamard and convolutional coding [for further details, see Codiga et al. (2004) and references cited therein]. The acoustic modem networking firmware is being developed for navy applications under the ongoing Seaweb initiative (Rice et al. 2001) and includes the protocols described in Codiga et al. (2004), augmented by an automatic repeat request (ARQ) mechanism as explained below.

b. Gateway buoys

In previously reported experiments the only gateway node was the existing United States Coast Guard (USCG) Montauk Point navigation buoy, which we equipped with a CDPD modem, an acoustic modem, and batteries powered by solar panels (Codiga et al. 2004). Such buoy-of-opportunity use has the advantage of leveraging the USCG maintenance effort, though it constrains the moored array to be near the existing navigation buoy. For the experiments reported here, a second project-dedicated relocatable gateway buoy was instrumented and deployed (Fig. 2). Its functional elements are similar to that found on the USCG buoy (shown in Fig. 4 of Codiga et al. 2004), though the electronics are housed in a sealed central well as opposed to a topside box, and the acoustic modem transducer is mounted at the base of the well instead of on a pole. Solar panels on the mast provide power (Fig. 2a). The main discus has \sim 1000 lb buoyancy, and the acoustic transducer is positioned \sim 3 m deep at the end of the extended-length well (Fig. 2b), in order to minimize interference by near-surface bubbles.

c. ADCP sensor nodes

ADCP nodes utilized custom firmware features, developed for this project, to pass a concise subset of the data stream to the acoustic modems for transmission while simultaneously recording full standard-format data internally (Codiga et al. 2004). ADCP sampling issues are detailed in Codiga and Houk (2002).

One ADCP sensor node (A6, below) did not generate a sufficiently long record either during WI02 or SP02 and is omitted from the analysis. During the WI02 deployment cruise, its acoustic modem transducer o-

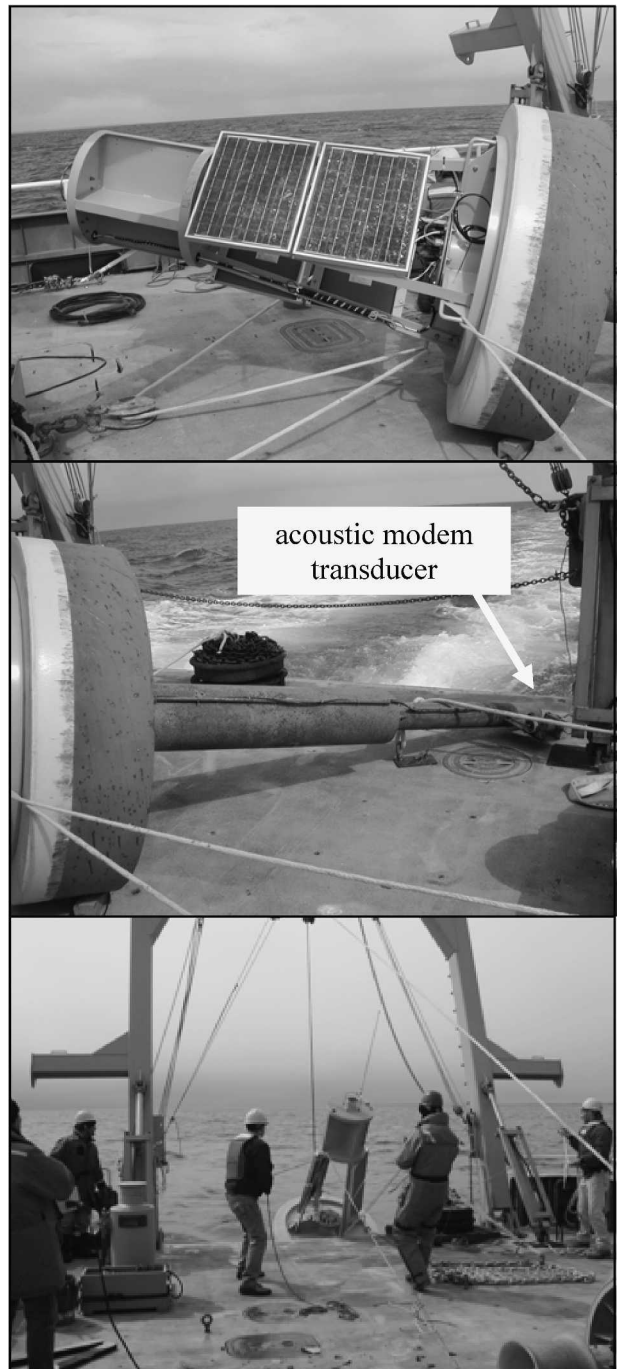


FIG. 2. Relocatable standalone gateway buoy, on its side on deck of R/V *Connecticut*: (a) upper mast portion (\sim 2 m high) with solar panels and sealed well containing acoustic modem and CDPD cellular modem electronics; and (b) subsurface portion, with extended base that positions acoustic modem transducer at depth \sim 3 m to limit interference by bubbles. (c) View during deployment.

ring failed nearly immediately; the bottom frame was recovered and redeployed with a spare replacement transducer, but fell silent again the day after the cruise. On recovery after WI02 the spare transducer was found to have also flooded, and the problem was traced to a manufacturing production issue. The ADCP collected good data internally, and the acoustic modem electronics attempted to transmit data as programmed, but the transducer did not emit nor detect any signals. Early in SP02, as described below, the node malfunctioned as a result of impact by trawling gear.

d. Sound speed profiles and winds

Two sources of hydrographic data are used to characterize the sound speed profile. First, an average profile was computed using data from each of three 1–2-day-long surveys with a towed undulating conductivity–temperature–depth (CTD) (30–31 January, 15–16 April, and 29–30 May) along repeat across-shore transects through the north–south leg of the moored array (Kirincich 2003). Second, a historical database of CTD casts (described in Ullman and Codiga 2004) from the region, marked by a dashed line in Fig. 1, was used to calculate monthly mean “climatological” profiles in 10-m vertical bins. Winds are from National Climate Data Center buoy 44025 (Fig. 1), as discussed in Codiga et al. (2004), and wind stress is calculated following Large and Pond (1981).

3. Moored array design and data routes

a. Configuration of moored array

The full FRONT4 acoustic communications network (Fig. 3) consists of 13 nodes: five ADCP sensors, one profiling video zooplankton sensor, five repeaters, and two gateway buoys. The five ADCPs include one central node (A7) and four at outlying points (A3, A6, A9, A12) that form a symmetric 10 km × 10 km cross. The plankton sensor (P13) is located near the center of the array. The five repeaters include one central node (R8) and four others (R4, R5, R10, R11), each 3 km from the center, which are in a symmetric ring roughly midway between the array center and the outer ADCP nodes. The gateways consist of the independently deployed standalone buoy (G2) at the array center, and the existing USCG navigation buoy adjacent to repeater R5 to the north and west of the array center.

Two separate sets of goals motivated the array design—one to achieve scientifically relevant oceanographic sampling, and one to demonstrate the networked acoustic modems for real-time data telemetry. From the standpoint of oceanography, the array meets

the following aims: O1) to sample both sides of a frontal region identified in sea surface temperature data of Ullman and Cornillon (1999); O2) to cover a region at least 10 km × 10 km, in part for data assimilative numerical modeling; and O3) to resolve both along-coast and across-coast spatial structure. The cross configuration is aligned such that one leg is 21° west of north to orient it perpendicular to the regional coastline that is set by the south shores of Long Island and Block Island.

To facilitate networked acoustic modem communications, the array achieves the following goals: C1) to incorporate the fixed USCG Montauk Point navigation buoy as a gateway node; C2) to include a second gateway, positioned near enough to shore to be within cellular telephone coverage, such that should one fail a single gateway can serve the entire array; C3) to have a repeater node adjacent to each gateway buoy, in order to always provide a direct acoustic path from the seafloor to each near-surface gateway acoustic modem; C4) to include a node no farther than 3 km away from each sensor; and C5) to provide a secondary route from each sensor to a gateway, for use should an individual node fail or be lost.

Goals C4 and C5 are constraints set by the choice of 3–4 km for maximum internode distance, or the range beyond which acoustic communications are not considered adequately reliable at this site. The appropriate internode distance is site and season specific, because it is dependent on a wide variety of factors that influence the acoustic channel, and is highly variable because of noise fluctuations and propagation effects. The internode distance that is used to design the array was based on initial field tests at this site (Codiga et al. 2004) that showed the range at which reliability fell to 50% was 3–4 km. On this basis, and given the fixed number of acoustic modems that are available for the project, the overall size of the array was limited to 10 km × 10 km. A larger array, ~18–20 km across based on a ~9 km internode distance, was originally proposed (see Fig. 1 of Codiga et al. 2004) based largely on the scientific advantages it could have (see O2). Based on the network performance described below, the optimal internode distance is smaller (larger) than 3–4 km in winter (spring). In this sense, by hindsight the choice of the 3–4-km internode distance for the array design was reasonable because the experiment spanned both seasons.

b. Routes and timing of network data transmissions

At the start of WI02, the routing tables (Table 1) set paths between each sensor and G2 that include at most three hops, or node pairs, between which the data packet is transferred along the route. The gateway for all nodes was G2, because G1 did not participate, as

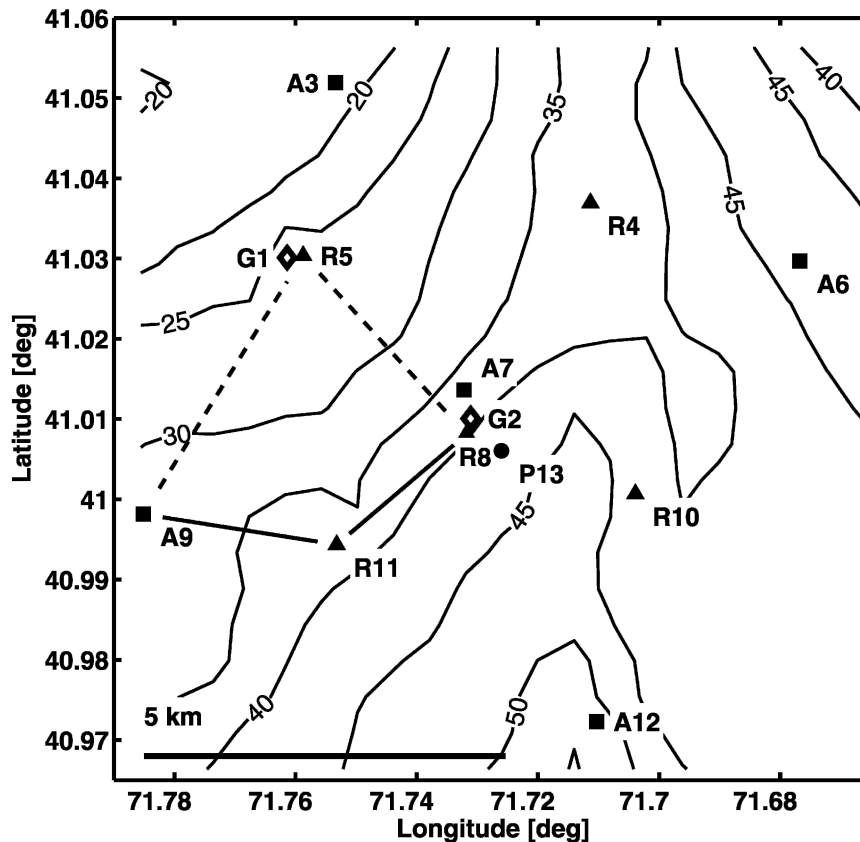


FIG. 3. Configuration of moored array with 13-node acoustic modem network. Area shown corresponds to inset in Fig. 1, with bathymetric contours marked in meters and 5-km distance marked at lower left. Open diamonds are the two gateway nodes: G1 on USCG Montauk Point navigation buoy, and standalone G2 buoy (Fig. 2). Solid symbols are sensor nodes: ADCPs with prefix A (A3, A6, A7, A9, A12) and moored profiling video plankton recorder (P13). Gray triangles are repeater nodes, prefix R (R4, R5, R8, R10, R11). As examples of network data routes (for complete list see Table 1), the routes from sensor node A9 are shown: primary (solid lines; A9 → R11 → R8 → G2) and secondary (dashed lines; A9 → R5 → R8 → G2).

described below. In Table 1 “horizontal” indicates that the hop is between two nodes about 3 km apart, both near the seafloor (except for R5 → G2, as marked); and “vertical” indicates a hop to the near-surface G2 node from a seafloor node (R8 or A7) within a few hundred meters. Routes in Table 1 are modified from originally planned routes (not shown) that (a) distributed traffic across the two gateways, and (b) distributed heavy traffic toward G2 across both R8 and A7 near the array center, which is a demonstration of the capability for A7 to act both as a sensor and a repeater (e.g., A7 would have acted as a repeater in A6’s route to G2); in light of a battery depletion issue for A7 that is described below, the routes used were those in Table 1.

No rerouting occurred during WI02. During the latter part of SP02, in response to unplanned events described below, the following routing changes were

made (using command sequences like those explained in Codiga et al. 2004) in real time from the shore:

- 1) On 1 May the route for A3 was changed to A3 → R5 → R8 → G2 in order to add R8. This was in response to a 2–3-day period in late April when no packets successfully crossed the R5 → G2 horizontal hop from a seafloor node to a near-surface node. The change meant that packets could reach the array center via the horizontal R5 → R8 hop between near-bottom send and receive nodes.
- 2) On 7 May, the route for A12 was changed to A12 → R11 → R8 → G2—a secondary route that replaces R10 by R11. This was in response to a ~3 day period during which R10 was silent, prior to which its battery voltage was noted to be near the unacceptably low level.

- 3) On 22 May, the route for A9 was changed to A9 → R5 → R8 → G2—a secondary route that replaces R11 by R5 (shown explicitly in Fig. 3). This was in response to the battery depletion of R11 relative to R5.
- 4) On 26 May the route for A12 was changed to A12 → G2. This was in response to the battery depletion of R11 and R8.

This is a time-division multiple access (TDMA) network. The schedule of data transmissions consisted of a regularly repeated cycle, during which each sensor transmitted data it collected during the most recent cycle. In WI02 (SP02) the cycle length was 80 (120) min. Transmissions from a given sensor were separated by at least 10 min from those of the other sources before or after it; thus, network collisions were avoided and network maintenance commands could be completed between scheduled transmissions. Typical data packet sizes were 100–300 bytes, which require about 3–8-s acoustic transmission time. The handshaking protocol can add an additional 2–60 s, depending on whether multiple attempts are required; most of the additional time consists of silent wait periods. In normal operation the network is, therefore, nearly always silent, with relatively infrequent transmissions occurring along a single route at a time. This is the main reason why an environmental impact statement assessing the project concluded that effects of the network on marine mammals are minimal.

4. Network deployment and function in response to unplanned events

For 3 months prior to FRONT4, in fall 2001, all of the sensors in the array were deployed without acoustic modems and recorded data internally only. During this time, for testing purposes, a subset of the acoustic modem network (R5, A7, P13, G2) was deployed and referred to as ForeFRONT4. The originally planned recovery–deployment sequence to follow ForeFRONT4 was designed to facilitate battery replacement at 3-month intervals, with instrument maintenance and repair (if necessary) as follows: 1) at the end of December 2001, recover all instruments for servicing; 2) in January 2002, start WI02 by redeploying the full array, including an acoustic modem at each node; 3) in mid-March, end WI02 by recovering the full array for servicing; 4) within 1 week, start SP02 by redeploying all instruments; and 5) in June, end SP02 with a full recovery. Several factors required these plans to be modified as the experiment progressed. Responses to these unplanned events illustrated the utility of redundancies

TABLE 1. Data routes in acoustic modem network throughout WI02 experiment and most of SP02 experiment. Horizontal hops are at ~3 km range between sending and receiving nodes, which are both located near the seafloor, except where noted.

Sensor	Full route	Individual hops	Type
A3	A3 → R5 → G2	A3 → R5 R5 → G2	Horizontal Horizontal, bottom to surface
A6	A6 → R4 → R8 → G2	A6 → R4 R4 → R8 R8 → G2	Horizontal Horizontal Vertical
A7	A7 → G2	A7 → G2	Vertical
A9	A9 → R11 → R8 → G2	A9 → R11 R11 → R8 R8 → G2	Horizontal Horizontal Vertical
A12	A12 → A10 → R8 → G2	A12 → R10 R10 → R8 R8 → G2	Horizontal Horizontal Vertical
P13	P13 → G2	P13 → G2	Vertical

and flexibilities incorporated in the network design and function.

a. Reliance on single gateway node: Unscheduled maintenance by USCG on the Montauk Point buoy

Unscheduled USCG maintenance on the Montauk Point navigation buoy equipped as G1 became necessary in late 2001. The USCG Cutter *Juniper* pulled the buoy, serviced it on deck, and redeployed it. This occurred on short notice, disallowing prior removal of the solar panels, cellular telephone modem, and acoustic modem that were installed for this project. As a result, damage to the instruments occurred. Attempts to repair and reinstall G1 were hampered by adverse sea conditions through WI02 and early SP02 experiments whenever schedules permitted visits, so G2 was the sole gateway. Redundancy of dual gateways in the array design, therefore, proved critical to the success of the experiment.

b. Temporary storage on gateway buoy: Gateway–shore link outage backup

The route from each sensor to the shore consists of two main segments—from the sensor to the gateway through networked acoustic modems, and from the gateway to the shore. The latter segment is a CDPD cellular modem connection and had numerous short (from a few hours up to more than a day) outages as a result of unpredictable cellular coverage dropouts. In nearly all cases, on reestablishing the link the missed real-time data were immediately retrieved from a stor-

age buffer in the gateway acoustic modem. On 14 February, during tests of software that was designed to automate the process of detecting cellular dropouts and reestablishing the link, a programming error made the CDPD modem inoperable. Data collection continued in the gateway storage buffer until 2 March when the buffer reached its capacity and, therefore, data collection for WI02 ended. In mid-March, at the start of SP02, the buoy was redeployed with a reprogrammed CDPD modem. The data from 14 February to 2 March were then retrieved from the gateway buffer in late March. The postrecovery analysis presented below treats this subset of data as if it arrived on shore in real time, as did the rest, with the intent to assess the subsurface acoustic modem network only while presuming perfectly reliable communications between the gateway and shore. Remote data retrieval from the storage buffer on the gateway acoustic modem thus served a key backup role in compensating for periods when the gateway–shore link was inoperable.

*c. Adaptive sampling and network rerouting:
Remotely from shore in real time*

The acoustic releases used in the ADCP sensor and repeater nodes failed at an unacceptably high rate in test deployments, and during ForeFRONT4 it became clear they could not be relied upon. This made remotely operated vehicle (ROV) recoveries necessary during WI02 and SP02, which were carried out by the North Atlantic and Great Lakes office of the National Undersea Research Center. Despite every effort to coordinate schedules on short notice, availability of the ROV team was limited, and difficult weather and current conditions meant recoveries did not occur when planned in certain cases. In terms of the results reported here, there were two main effects. First, the node A7 that was deployed for ForeFRONT4 in September 2001 was not recovered and serviced until the end of WI02 in March 2002. This caused an unplanned extension of the deployment by some 3 months, roughly a factor of 2, making battery depletion a risk. To keep both the ADCP and acoustic modem functioning reliably for the full extended-deployment duration, commands were sent to them via the acoustic communication network. The ADCP was reprogrammed to sample with fewer pings and to transmit a smaller subset of the data through the acoustic modem. These changes reduced power consumption by both instruments. This is an example of the capability of the network for adaptive sampling, or interactively changing instrument settings in real time from shore.

A second impact of having no reliable acoustic releases was that the five repeater nodes were deployed

in January and not recovered until well after the end of the SP02 experiment more than 6 months later, instead of being serviced each 3 months as planned. This was a result of prioritizing the repeaters lower than the sensor nodes during recovery cruises, which was a necessity given the limited number of ROV dives that were available. Batteries that were provided to each node were sufficiently conservative so that for some repeaters they held up through nearly all of both WI02 and SP02 without servicing, while for others depletion occurred prior to the end of the experiment. Acoustic modem battery voltages can be polled from the shore in real time via the acoustic network and were monitored periodically throughout the experiment. When battery depletion occurred data routes were reconfigured remotely from shore in real time (see previous section) to bypass the depleted node. This is another demonstration, in addition to that described in Codiga et al. (2004) when a repeater node was trawled out, of the flexibility to change data routes in real time.

*d. Real-time reprogramming to react to trawling
impact on sensor*

Sensor nodes were hit by trawlers, and in two cases this impacted planned data collection. In both cases the trawl-resistant frames succeeded, despite that the sensors did not record useful data following the impact, in the sense that the instruments were recovered for use in later deployments whereas they may have otherwise been lost or destroyed. First, node A12 was struck within a week of being deployed for WI02. From shore in real time, it was known only that the node had fallen silent. During recovery in March, the ball float in its bottom frame was found to have been shattered. Postrecovery, internally logged ADCP data revealed a sharp discontinuity in pitch and roll angles on 23 January, implicating the impact of dragged gear. After the impact, the ADCP neither recorded any data nor provided any to its acoustic modem for transmittal. The second trawling impact struck node A6 less than 2 weeks after the start of SP02. In real time, a series of frequent acoustic transmissions of unexpectedly small size were heard from A6. Attempts were made to reset and reprogram the ADCP remotely, without success, and within a day the node fell silent. During recovery in June deep scrapes in the aluminum-bottomed frame were apparent, which could only have been caused by heavy dragged equipment, and the acoustic modem batteries were fully depleted. Postrecovery inspections indicate that on 4 April the ADCP stopped recording useful data and caused the acoustic modem to broadcast a series of redundant packets, draining its batteries in a 1-day period. The attempts to reprogram the

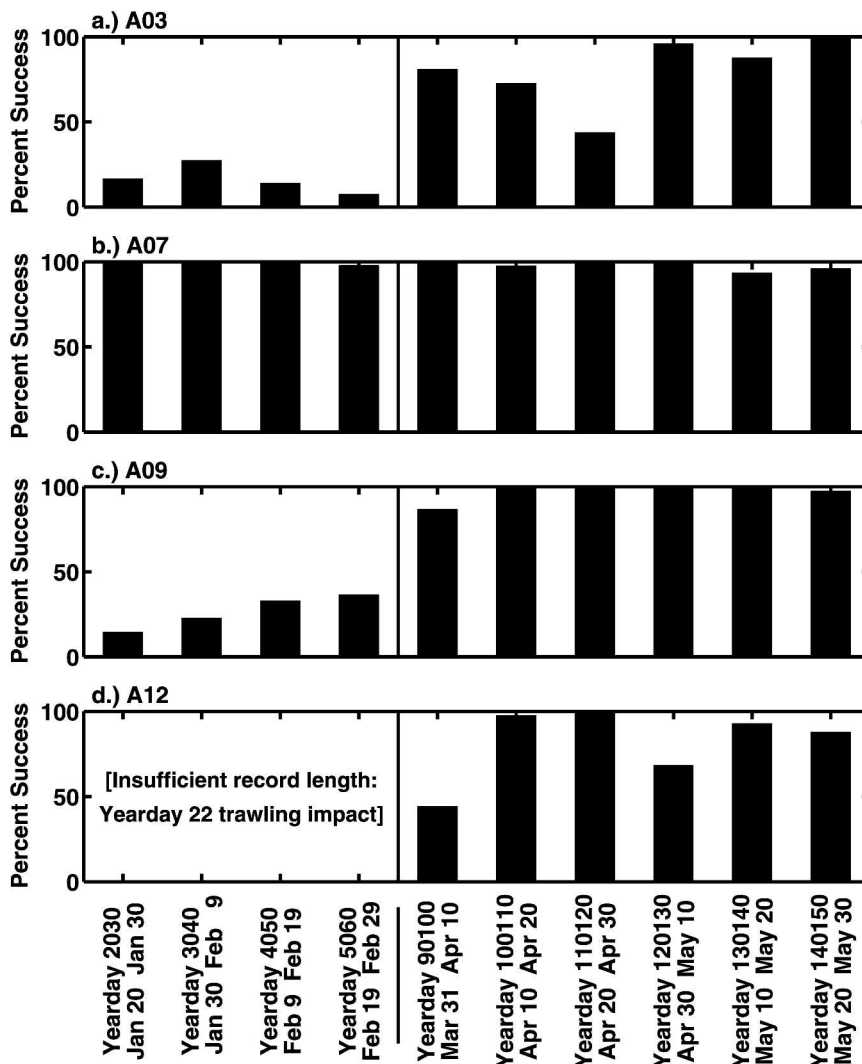


FIG. 4. Bulk performance of entire acoustic modem network during ~6 week WI02 experiment (left four bars) and ~9 week SP02 experiment (right six bars), based on the percent of successful arrivals of ADCP sensor transmissions during successive 10-day intervals. Performance is consistently very reliable for node A7, which has a one-hop route and is situated adjacent the gateway. Percent successes of other nodes, utilizing multiple-hop routes to reach the gateway from 5 km away, are low during WI02, then rise appreciably between the end of Feb and early Apr, and subsequently remain higher on average.

ADCP in real time from shore, though unsuccessful in this instance, demonstrated the network capability to assist in reacting to a trawling incident.

5. Results: Bulk performance of networked acoustic modems

Bulk performance of the network as a whole consists of the net successful delivery of data from each sensor to shore in real time, without regard to routing issues or details of acoustic modem configurations, such as the

handshaking protocol. The bulk percent of successful transmissions have been calculated for individual sensors during each of a sequence of consecutive 10-day intervals spanning both WI02 and SP02 (Fig. 4 and Table 2). The most reliable sensor during WI02 and SP02 from January through June was the central ADCP, A7, which was located adjacent to the gateway buoy G2 (Fig. 4). Its route is one hop: a nearly vertical and, therefore, almost certainly direct, acoustic path. Its 10-day success rate typically exceeded 99% and was more than 97% throughout the entire duration of both

TABLE 2. Values of bulk performance (see Fig. 4) as percent successful arrivals. Values in italics are cumulative summaries.

	Interval (yearday 2002)	A3	A7	A9	A12
	20–30	16.7	100	14.4	—
	30–40	27.2	100	22.8	—
	40–50	13.9	100	32.8	—
	50–60	7.4	97.8	36.4	—
All WI02	<i>20–60</i>	<i>16.3</i>	<i>99.5</i>	<i>33.8</i>	—
	90–100	80.8	100	86.7	44.2
	100–110	72.7	97.5	100	97.4
	110–120	43.7	99.2	99.2	100
	120–130	95.8	100	99.2	68.3
	130–140	87.5	93.3	100	92.9
	140–150	100	95.8	97.4	87.8
All SP02	<i>90–150</i>	<i>80.1</i>	<i>97.6</i>	<i>97.1</i>	<i>81.8</i>

WI02 and SP02 (Fig. 4b). The performance of node P13 (not shown), the route for which is a similar single nearly vertical hop, was comparable to that for A7.

During WI02 (left side, Fig. 4), A3 and A9 had 10%–35% successes, which are markedly lower than that of A7. These nodes had multiple-hop routes (Table 1) that included internode distances of at least 3 km. (Node A12 did not return a sufficiently long record for inclusion in the WI02 analysis, due to a trawling impact as described above.) During SP02 (right side, Fig. 4) sen-

sors with multiple-hop routes (A3, A9, and A12) saw markedly improved percent success over that in WI02. For A9, successes had risen to more than 80% in April and were maintained through May at more than 90%. For A3 and A12, successes were between 40% and 100% during SP02, averaging about 80%, with the lower-than-average values all occurring before mid-May. During March there is clearly a transition toward improved performance across the horizontal hops.

6. Sound speed profiles and acoustic ray paths

Averaged sound speed profiles from towed-body CTD surveys in 2002 (Fig. 5, asterisks, crosses, plusses) span a range of upward- and downward-refracting conditions. Underlying processes controlling the seasonal cycle of temperature and salinity profiles are discussed by Ullman and Codiga (2004). The 30–31 January survey reveals upward refraction, the 15–16 April survey shows a nearly vertically uniform sound speed with a weak middepth minimum, and the 29–30 May survey is downward refracting. These results are consistent with the seasonal progression seen in climatological sound speed profiles (Fig. 5, solid symbols)—upward refraction during January and February changes to a nearly constant speed profile in March and April and progresses to increasingly stronger downward refraction

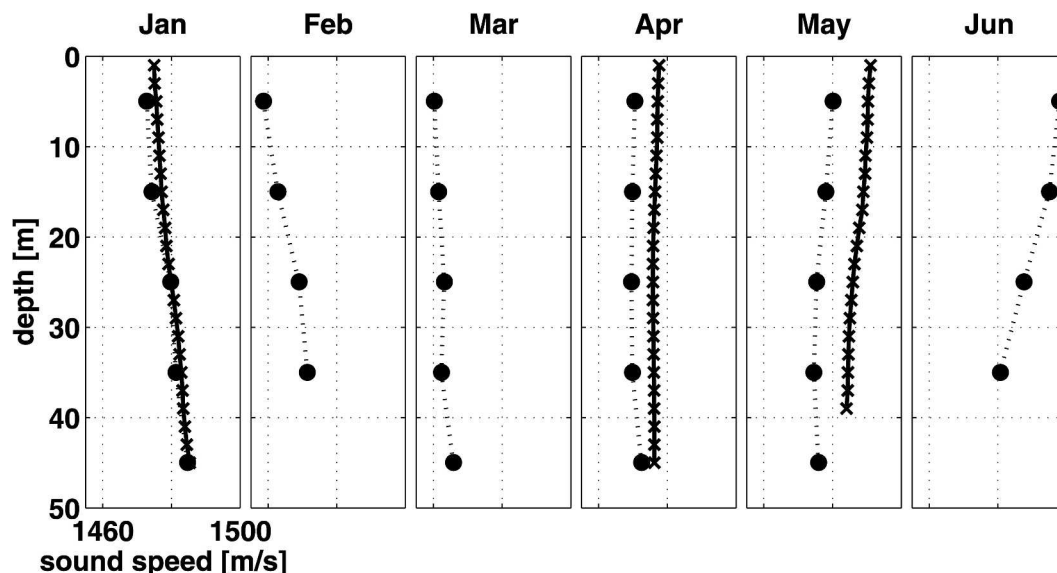


FIG. 5. Sound speed profiles. Three curves (Xs with solid lines, shown in Jan, Apr, and May frames) are averages across 1–2-day surveys (30–31 Jan, 15–16 Apr, and 29–30 May, respectively) by towed undulating CTD (Kirincich 2003) that repeated a transect aligned with A3–A7–A12 of the moored array. Solid circles with dashed lines show climatological data from Jan to Jun, the months the field experiments spanned: monthly mean profiles, binned in 10-m intervals, from historical database (described in Ullman and Codiga 2004) of CTD profiles within the dashed box in Fig. 1. In 2002 as well as the climatology, winter conditions are upward refracting, and following a Mar/Apr transition spring conditions are downward refracting.

through May and June. The January and April 2002 profiles show higher sound speed magnitudes than climatological values. This is due to temperatures that were anomalously warm in 2002. However, upward-refracting conditions waned in late March or early April of 2002, just as they do in the climatological cycle.

Numerical ray-tracing calculations incorporating the three sound speed profiles measured in 2002 and representative bathymetry indicate strongly contrasting acoustic paths (Fig. 6). In late January, upward refraction causes ray paths between nodes at ranges of a few kilometers to interact with the air–sea interface multiple times. In April, a more nearly downward-refracting profile reduces reflections off of the sea surface. In June, the fully downward-refracting profile enables paths between seafloor nodes at large ranges to exist with bottom reflections but no sea surface interaction.

It is clear that improvement in the bulk performance of horizontal hops between late February and early April (Fig. 4) is associated with sound speed profile changes from upward to downward refraction (Fig. 5). As spring progresses, the acoustic channel permits rays in horizontal hops (Fig. 6) to interact less with the sea surface, where they can be distorted and scattered by the rough surface, as well as absorbed by bubbles. Below we consider the influence of winds, which contribute to packet corruption by roughening the air–sea interface and by increasing the ambient noise level, which reduces the signal-to-noise ratio. Weakening of winds from winter to spring is expected to improve spring performance, in addition to increasingly downward-refracting conditions.

7. Time series: Wind effects and individual hop statistics

Time series of the data packets that are received (Fig. 7 for WI02; Fig. 8 for SP02) by the gateway, operating in the receive-all mode as described next, illustrate the relationship of horizontal link performance to winds, including individual hops within multiple-hop routes. In the receive-all mode the gateway receives data packets whether they are traveling 1) on the last hop in a route, so the gateway is their immediate destination; or 2) on a hop from earlier in the route, between two nodes other than the gateway, in which case the gateway in effect “overhears” (without involvement of the handshaking protocol described below). In favorable propagation conditions, the same data on an n -hop route can, thus, result in n redundant gateway receipts, while a less clear channel may mean that the gateway receives the packet only from the last node in the route. When the

channel is clear enough for a transmission from an upstream, or more distant, node to be received by the gateway, it will then typically be received from all of the remaining downstream nodes. However, in an acoustic channel with complex ray paths due to, for example, bathymetric features and/or horizontally varying sound speed, one or more upstream transmissions can be received by the gateway while subsequent downstream transmissions are not.

Network reliability decreases in association with strong winds during both WI02 and SP02 (Figs. 7, 8). During WI02 the wind stress magnitude commonly exceeded 0.1 N m^{-2} for several-day periods, while during SP02 such stresses were less frequent and generally lasted for shorter periods. In WI02 (Fig. 7) winds disrupt data arrivals from A3 and A9, whose routes involve horizontal hops, for up to a few days at a time. Recall that simultaneously the vertical A7 → G2 hop was very reliable (Fig. 4). The straightforward interpretation based on Fig. 6 is that vertical hops can occur along direct acoustic paths without reflection off of the roughened sea surface, which is not true of horizontal hops. During the generally weaker winds (Fig. 8) and the downward-refracting sound speed profile (Fig. 5) of SP02, disruptions of horizontal hops are less common than in WI02, which is again consistent with ray paths (Fig. 6) interacting less with the sea surface. The effect of a higher ambient noise level associated with strong winds should also increase reliability during spring relative to winter. However, even in spring conditions strong winds impeded communication for brief intervals along nearly all routes, including the short vertical hop of R8 → G2.

Statistics of receipts by the receive-all gateway from individual nodes in multiple-hop routes (Table 3 for WI02; Table 4 for SP02) reveal certain general patterns. Percentages are relative to the total number of unique packets that are successfully delivered from the sensor throughout WI02 (Table 3), and through SP02 until rerouting began (Table 4). A specific example provides context for the values in the table. For A3 in WI02, the sensor transmitted 784 packets and 184 were received successfully by the gateway at least once, regardless of their route, for a bulk percent success (e.g., Fig. 4) of 19%. The values in the table show that of those 148 packets, 73.6% were received directly from the nearest node (R5, at a range of ~ 3 km) and 50.7% were received directly from the sensor node itself (A3). This is consistent with diminished propagation, reducing gateway receipts from more distant nodes; the values do not sum to 100% because in 24.3% of the deliveries redundant transmissions from both R5 and A3 were received. Furthermore, this example illustrates that the receive-

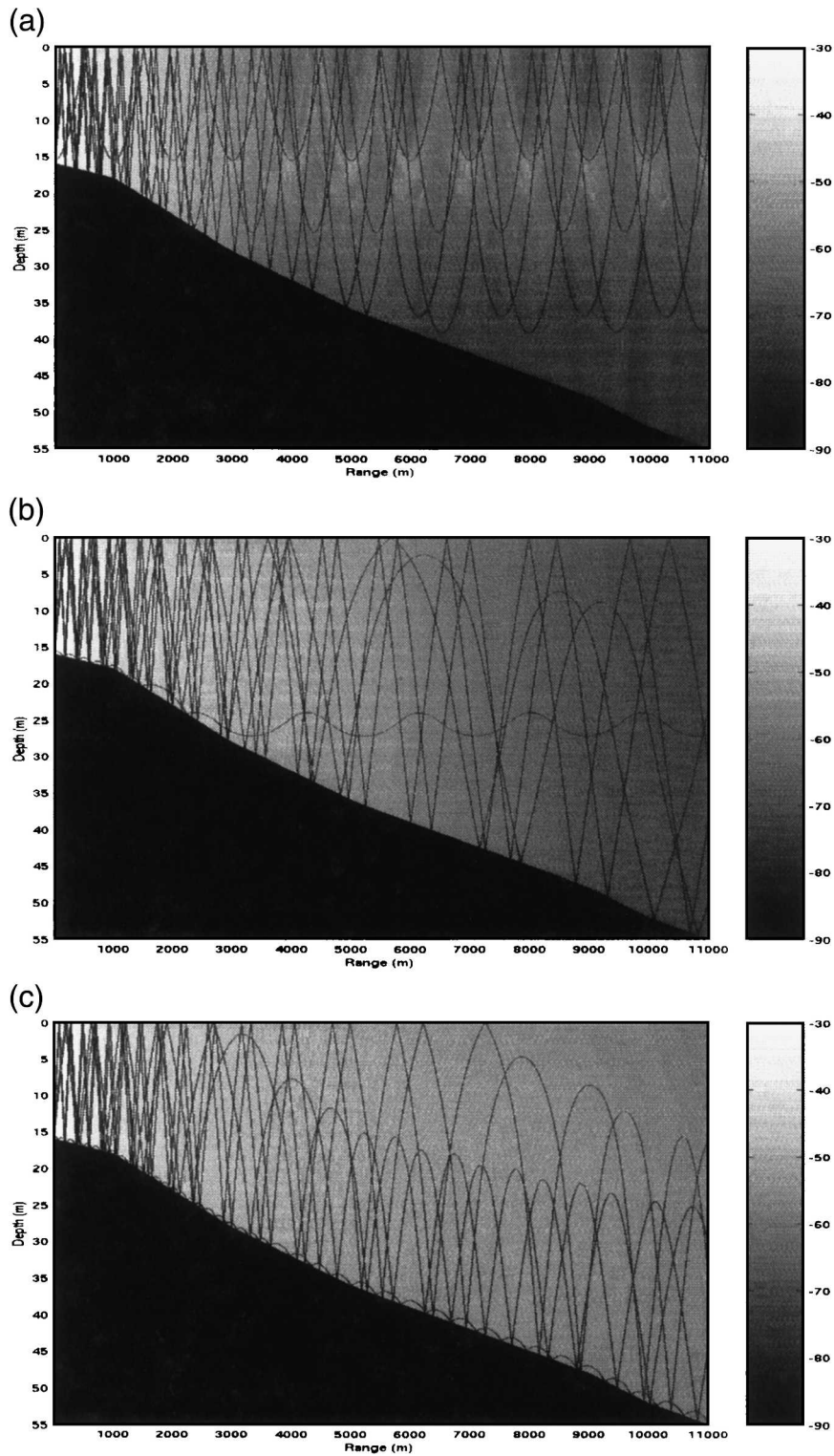


FIG. 6. Numerically modeled acoustic ray tracing for topography representative of an across-shore transect through nodes A3, A7, and A12 of the network (Fig. 3). Sound speed profiles are from 2002 surveys as shown in Fig. 5 for (top) Jan, (middle) Apr, and (bottom) May. Source is 0.5 m off of the bottom at the left, with rays launched at a range of angles. Grayscale shows acoustic power (dB) relative to the source level. Over ranges of several kilometers, ray interactions with the sea surface are more numerous and power loss at a given range is more severe in winter than in spring.

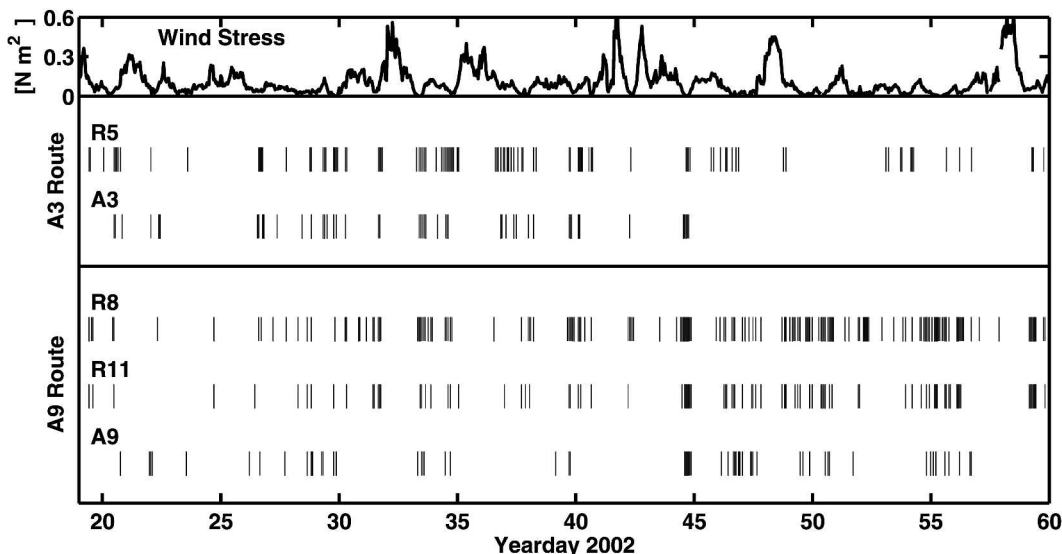


FIG. 7. Time series receipts by gateway G2, in receive-all mode, of packets sent from individual modems along multihop routes during WI02. Wind stress at 44025 buoy (see Fig. 1) shown at top.

all mode substantially increases the bulk success; were the receive-all mode not implemented the net successes would have been 73.6% as high. Aspects of multihop statistics (Tables 3 and 4) indicate complex ray paths, particularly in WI02. For 26% and 12% of deliveries from A3 and A9, respectively, in WI02, the transmission from the 5-km range succeeded while that subsequently from 3 km did not.

The percentage of time that all hops on a route are received by the gateway can be used to gauge how appropriate the internode distance of the array is with respect to the channel conditions. When the percentage is relatively low, such as in WI02 (Table 3), the internode distance of the array may be longer than optimal, and repeaters and multiple hops are critical to increasing the bulk success rate. The extent to which the percentage increases in SP02 (Table 4) is an indication that repeaters are relied upon less; the array could then function nearly as well without them, or, alternatively, with a larger internode distance, such that the same combination of nodes could span a larger region. In SP02 an internode distance of 5 km would not have been unreasonable, based on the reliability seen at this range (Table 4).

8. Importance of handshake protocol

This section assesses performance of the handshake protocol between node pairs. A record logged internally by the node A9 acoustic modem is used, whereas up to this point the analysis has been entirely based on data recorded by the gateway in the receive-all mode.

Data transmission across each node pair in a network route occurs via a handshake protocol, not as a single blindly sent packet. The sending node initiates with a short “request to send” (“RTS”) utility packet. On receipt of the RTS, the receiving node replies with a short “clear to send” (“CTS”) utility packet. If the sending node has not yet received CTS it will resend RTS up to a programmable number of times (4 times in this experiment). The sending node will transmit the data packet only upon receipt of the CTS. If the receiving node has sent a CTS but has not successfully received the data packet, it sends a short ARQ packet up to a programmable number of times (2 times in this experiment). In response to ARQ, the sending node retransmits the data packet. The handshake, therefore, consists of two main elements: RTS–CTS, which allows for multiple attempts to establish a link before sending data, and ARQ, which permits multiple attempts to send the data packet should the first not be received uncorrupted. Each attempt to deliver data across the node pair results in a sequence of RTS, CTS, data, and ARQ packets. For a perfectly clear channel, the sequence is RTS–CTS–data, or symbolically, RCD. For a very adverse channel, four RTS packets are sent and there is no response, or RRRR. Numerous other sequences are possible, such as RRCDAD, in which the RTS was resent once and one ARQ was necessary.

The present aim is to determine, for a 3-km hop between near-seafloor nodes, (a) to what extent the handshake improves successes, and (b) to what extent the improvement results from RTS–CTS or ARQ. The focus is the A9 → R11 hop for 54 days during WI02, a

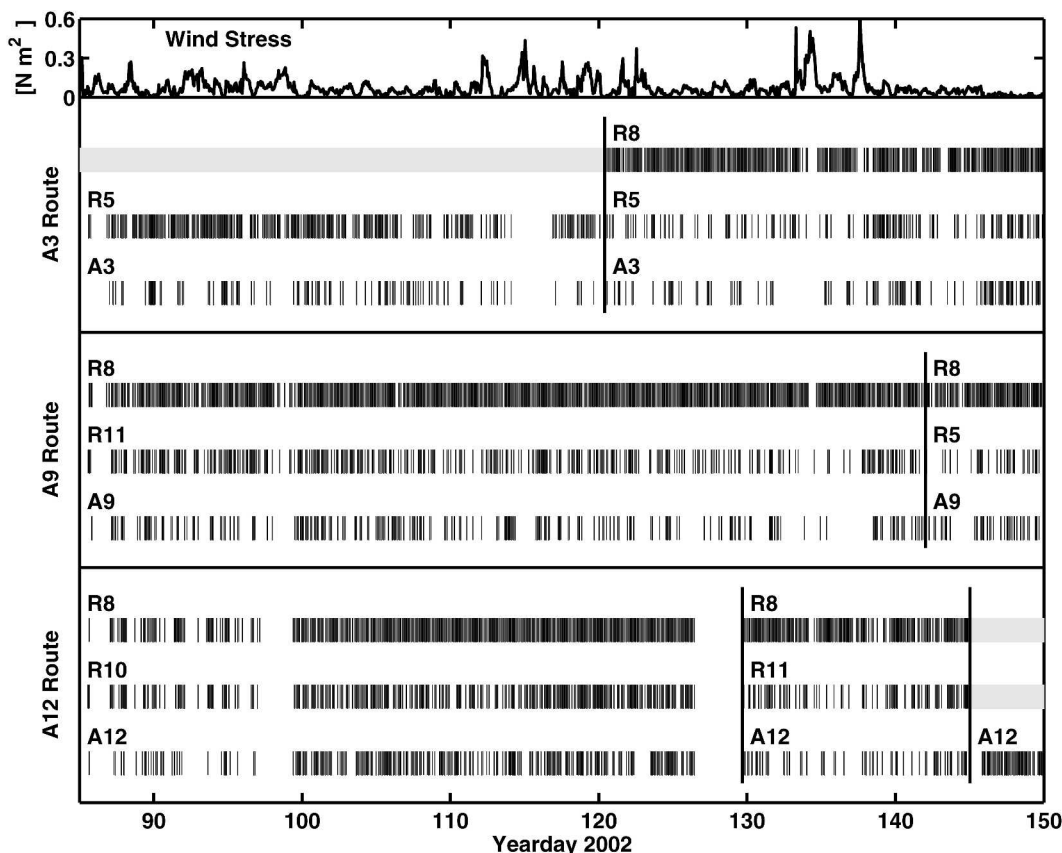


FIG. 8. As for Fig. 7, but for SP02. Gray bars indicate nodes that are not included in the route.

period when the sound speed profile and wind effects that are described above resulted in poor performance. This is a good test for the handshake protocol, because it is not as important when the channel is clear. This is the first report on field performance of the combined RTS-CTS and ARQ in FRONT4 deployments. Previous tests (Codiga et al. 2004) with only RTS-CTS active showed it to be useful, but were limited due to reliance on receive-all gateway records only, which are not well suited to address bottom-to-bottom hops in adverse channel conditions.

Of 964 attempts to send data from A9 to R11, 40% were successful. Among the successful attempts, 43% were RCD; for this analysis these will be considered to represent handshake-independent performance, in effect, that which is achievable by a handshake-free blind-data transmission, because retries by neither RTS nor ARQ were involved. Thus, 57% of the successes involved a retry and would have failed without handshaking. These handshake-dependent successes can be partitioned in to three groups (Table 5): 53% were due to ARQ retries only, 30% were due to RTS retries only, and 17% were due to both.

The handshake protocol is, therefore, critical to the bulk performance of the network, given that reliability of this seafloor-to-seafloor link improved by more than a factor of 2 during a period when the channel was adverse. Furthermore, while both RTS-CTS and ARQ resulted in improvement, the latter was more important.

TABLE 3. Statistics of successful packet arrivals at the gateway from individual nodes along multiple-hop routes during WI02, based on the receive-all gateway record (see Fig. 7). Values in the final two columns are percentages relative to bulk successful receipts from the corresponding sensor.

Sensor	Bulk successful receipts (%)	Node along route	Range (km)	Total	Received from only this node
A3	16.3	A3	5	50.7	26.3
		R5	3	73.6	49.3
		Received by all nodes		24.3	
A9	33.8	A9	5	29.0	12.6
		R5	3	45.3	3.7
		R8	0.2	82.7	38.3
		Received by all nodes		11.7	

TABLE 4. As for Table 3, but during SP02 (see Fig. 8) prior to the 1 May routing change (hence, bulk success values differ from those in last column of Table 2).

Sensor	Bulk successful receipts (%)	Node along route	Range (km)	Total	Received from only this node
A3	65.7	A3	5	36.1	4.6
		R5	3	95.4	63.9
		Received by all nodes		31.6	
A9	95.3	A9	5	38.6	1.5
		R5	3	58.2	0.5
		R8	0.2	98.8	29.4
		Received by all nodes		25.9	
A12	80.5	A12	5	61.1	4.8
		R10	3	70.4	0.3
		R8	0.2	94.6	15.0
		Received by all nodes		46.1	

9. Discussion

The capabilities that were demonstrated by the network are relevant in the context of plans developing for the coastal component of a Global Ocean Observing System (C-GOOS; e.g., Malone and Cole 2000) to provide data streams for operational and scientific uses.

Data collected in real time were distributed at a project Web site (Fig. 9; online at <http://nopp.uconn.edu/ADCP/index.html>) where time series of current vectors at a range of depths spanning the water column were presented graphically for user-selectable time periods. Surveys of operational users of real-time data, for example, in navigational or fishery applications, indicate that bottom temperature and wave conditions are among the most sought information (Piasecki et al. 2003). The ADCPs in this project measured the former and could collect the latter as well with only a change in firmware.

The ability for networked acoustic modems to serve arrays spanning larger regions without including impracticable numbers of repeaters rests on improving reliability at ranges larger than 5–6 km. In this regard directional acoustic modem transducers that can be remotely steered electronically, presently under development (Butler et al. 2003), appear to hold promise. As noted by Codiga et al. (2004), a store-and-forward modem capability would help limit the impact of reduced network reliability in winter.

The wireless nature of the network and its reliance on a relatively small number of buoys serving a larger number of sensors make it well suited, in general, for areas where fishing and shipping activities make sea-

TABLE 5. Statistics of handshake-dependent exchanges on the A9 → R11 hop, during 54-day period commencing at the start of WI02. Based on internally recorded acoustic modem buffer from node A9.

	No. of occurrences	Percent of handshake-dependent successes
Relied on ARQ only (total)	118	53%
RCDAD	79	
RCDADAD	39	
Relied on RTS-CTS only (total)	66	30%
RRCD	45	
RRRCD	17	
RRRRCD	4	
Relied on ARQ and RTS-CTS (total)	38	17%
RRCDAD	16	
RRCDADAD	11	
RRRCDAD	7	
RRRCDADAD	4	
RRRRCDAD	1	
RRRRCDADAD	3	

floor cabling and buoy maintenance impractical (Fig. 10). In future applications, an Iridium connection between the gateway and shore, instead of CDPD, could overcome the constraint of maintaining the gateway within cellular telephone coverage nearshore. This would enable an array to be positioned, for example, near the shelf break or in a remote area without extensive cellular coverage. Furthermore, gateways need not be buoys, but instead can be autonomous underwater vehicles (AUVs), equipped with an acoustic modem, that surface for CDPD or Iridium communication. There is clearly potential for command and control of the AUV from shore via the fixed network nodes. An AUV gateway removes the buoy maintenance effort as well as potentially sampling water column hydrographic variables that are, at present, inaccessible to sensors in trawl-resistant bottom frames. For the latter aim, a buoy gateway has the advantage that moored vertically profiling hydrographic sensors (e.g., Codiga et al. 2002) can operate along its wire (Fig. 10).

The scientific value of a long time series collected by spatially distributed instruments is well established regardless of the real-time nature of the data streams. ADCP records from this experiment supported investigation of oceanographic processes from seasonal (Ullman and Codiga 2004; Codiga 2005) to tidal (Codiga and Rear 2004) time scales, and provided context for numerical modeling of circulation (Edwards et al. 2004a) and related data assimilation techniques (Edwards et al. 2004b).

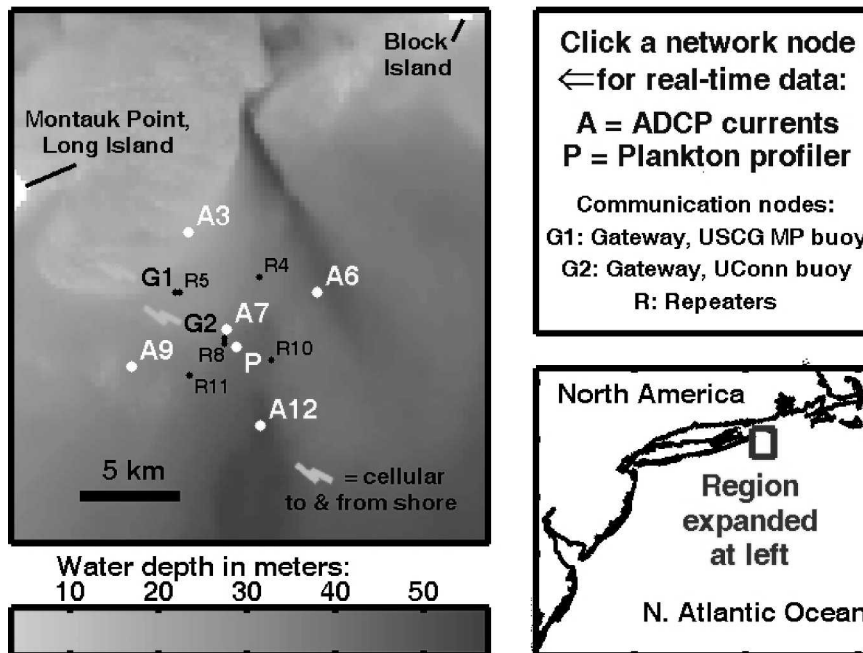


FIG. 9. User interface for Web-based display of real-time data.

10. Summary and conclusions

The application of networked acoustic modems to real-time wireless telemetry of data from an array of moored ADCPs in the coastal ocean has been demonstrated. In the winter and spring of 2002 the array and network sent data from a 10 km \times 10 km region to shore nominally several times a day, as motivated by typical needs for data assimilative modeling of coastal processes. The experiment site, the inner continental shelf off of Montauk Point (Figs. 1 and 3), was selected in part for its heavy trawl fishing and shipping traffic. This is a challenge for real-time data collection because seafloor cabling and/or maintenance of a surface buoy for each oceanographic sensor in a moored array are problematic. A network of acoustic modems is well suited to overcome these impediments. Here, one scientific buoy (Fig. 2) was deployed and acted as a gateway for communication between the shore and several instruments that were distributed across the moored array, and a similarly equipped USCG navigation buoy served as a backup gateway.

The flexibilities and redundancies built in to the design of the moored array and acoustic communications network were demonstrated in response to several unplanned events during the course of the experiment. Network data pathways were reconfigured to rely solely on one gateway, instead of both, when unscheduled USCG maintenance made the navigation buoy gateway unavailable. Temporary losses of CDPD com-

munication between the gateway and shore, for example, due to cellular telephone network outages, were compensated by the ability to retrieve data out of a storage buffer in the acoustic modem on the gateway buoy upon reestablishing the CDPD connection. Adaptive sampling, or changing operating parameters of oceanographic sensors in real time from shore, was demonstrated. In this case sampling parameters were modified in order to limit the battery depletion of instruments that had to remain deployed for longer than planned due to unreliable acoustic releases. For this same reason certain nodes failed due to battery depletion, and the remote rerouting of network data paths that was carried out in real time extended the successful data collection. Finally, attempts to reprogram one node, though unsuccessful, were made remotely in real time in response to malfunctions that were caused by the impact of trawling equipment. Trawl-resistant bottom frames made possible azimuthally omnidirectional signaling of the acoustic modems that they housed, as is necessary to facilitate real-time changes to network routing. They also resulted in the successful recovery of all ADCPs, despite multiple incidences of trawling impacts.

Bulk performance of the acoustic network (Fig. 4 and Table 3) improved substantially during the progression from winter through spring. While data from the seafloor sensor adjacent the gateway were delivered more than 97% of the time through both seasons, deliveries

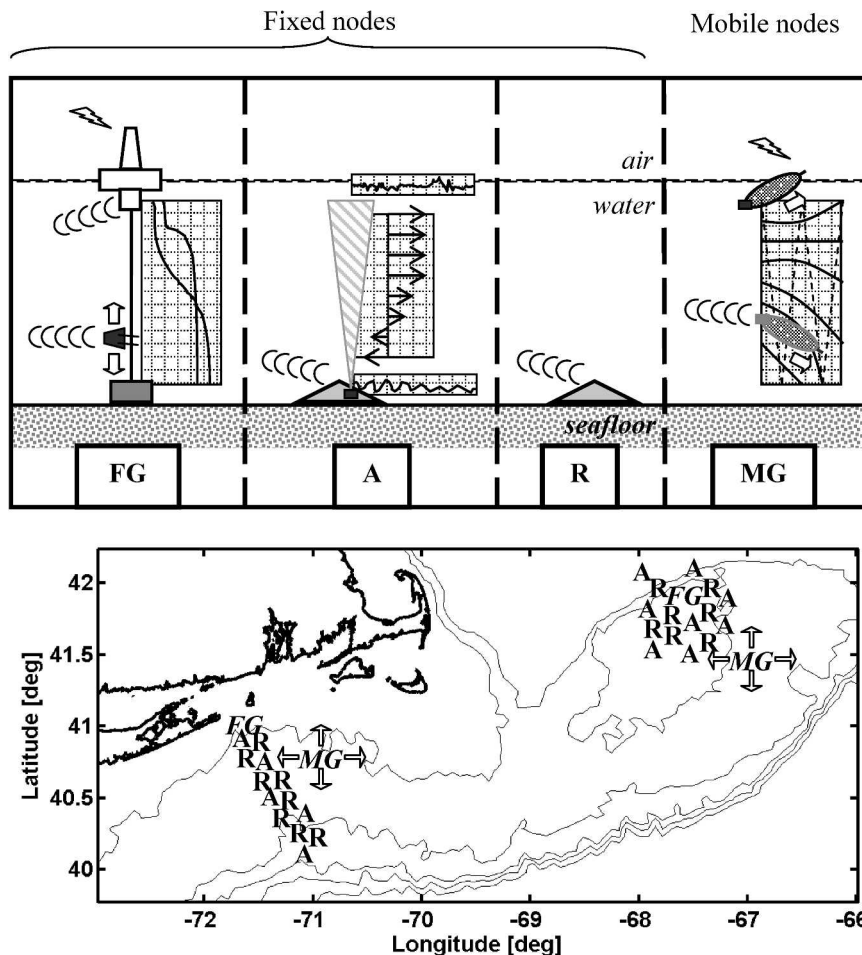


FIG. 10. Schematic of potential future application of networked acoustic modems as a component of C-GOOS. The nominal 15-km internode distance used is likely to be supported by range-enhancement measures now in development, such as electronically steerable directional transducers. (top) Elements of network using proven technology, the three types of fixed node and one type of mobile node: fixed gateway “FG” is a combined gateway/sensor, a buoy with surface gateway, and profiling sensor node on the wire to collect time series vertical profiles of hydrographic variables; “A” is trawl-resistant bottom frame with ADCP to collect time series of surface wave parameters, current profiles, and bottom temperatures; “R” is repeater node housed in trawl-resistant bottom frame; mobile gateway “MG” is combined gateway/sensor, an AUV equipped as a gateway when it surfaces and with sensors to map hydrographic variables vertically and horizontally, for which command and control could in principle be carried out from shore via the fixed network nodes. (bottom) Schematic arrays off of the northeast coast of North America, with 50-, 100-, 250-, 500-, and 1000-m isobaths shown. Nearshore FG within cellular telephone coverage uses CDPD modem, and FG farther offshore uses Iridium with satellite service.

from the nodes that were separated horizontally from the gateway by 5 km showed average reliability of 25% (86%) in winter (spring). The seasonal cycle in the sound speed profile includes a transition, typically in March, from wintertime upward refraction to springtime downward refraction (Fig. 5). This requires that acoustic ray paths between horizontally separate nodes reflect off the sea surface much less in the spring, when

direct acoustic paths may be possible, than in the winter when they are not (Fig. 6). Wind roughens the air–sea interface and increases ambient noise, and, therefore, has a seasonal cycle that also acts to degrade winter performance more so than spring (Figs. 7 and 8). As guided by previous measurements (Codiga et al. 2004), the array was designed for a 3–4-km maximum internode distance, or the range beyond which acoustic com-

munications is not considered to be adequately reliable. Based on observed performance as a function of range (Tables 3 and 4), a 1–2-km internode range would be more optimal during winter, while spring conditions could support node separations up to 5–6 km.

Several features of acoustic modem firmware were critical. Receive-all gateway mode increases bulk success rates by enabling the same data packet to arrive at the gateway redundantly. As expected, this caused the most improvement during winter, when the acoustic channel was most complex, even causing routes between nodes at larger ranges to sometimes be more reliable than those closer together. A handshake protocol incorporating two types of resending opportunities (RTS–CTS and ARQ) nominally doubled the reliability of individual hops when the channel was adverse, with ARQ being the more important contributor (Table 5).

The main finding is that networked acoustic modems are a proven means for real-time data collection from instruments that are distributed across areas of the coastal ocean. The system that is demonstrated here is particularly useful where cabling and multiple surface buoys are not feasible. A publicly accessible Web site with graphical presentation of user-selectable time series data in real time was developed (Fig. 9). In this context, networked acoustic modems are well suited to form a communications backbone for a component of coastal ocean-observing systems (Fig. 10).

Acknowledgments. We thank, in particular, those involved in the demanding fieldwork and custom instrument design and preparation: Captain T. Cabaniss, D. Nelson, and the R/V *Connecticut* crew; D. Arbige, D. Cohen, R. DeGoursey, R. Dziomba, J. Godfrey, G. Grenier, A. Houk, and L. Rear of the University of Connecticut Marine Sciences; I. Babb, P. Boardman, C. Bussell, and N. Worobey of NURC-NAGL; B. Creber and C. Fletcher of SSC-SD; T. de Groot, J. Hardiman, D. Porta, and K. Scussel of Benthos. T. Fake coded the real-time Web display. D. Ullman prepared the climatological hydrographic data. This work was sponsored by Office of Naval Research Award N00014-99-1-1020 through the National Ocean Partnership Program. Cost sharing for involvement of U.S. Navy personnel was provided by ONR 321SS and by the SSC San Diego Seaweb Initiative.

REFERENCES

- Butler, J. L., A. L. Butler, and J. A. Rice, 2003: A tri-modal directional transducer. *J. Acoust. Soc. Amer.*, **115**, 658–665.
- Codiga, D. L., 2005: Interplay of wind forcing and buoyant discharge off Montauk Point: Seasonal changes to velocity structure and a coastal front. *J. Phys. Oceanogr.*, in press.
- , and A. E. Houk, 2002: Current profile timeseries from the FRONT moored array. Department of Marine Sciences, University of Connecticut Tech. Rep., 19 pp.
- , and L. V. Rear, 2004: Observed tidal currents outside Block Island Sound: Offshore decay and effects of estuarine outflow. *J. Geophys. Res.*, **109**, C07S05, doi:10.1029/2003JC001804.
- , D. S. Waliser, and R. E. Wilson, 2002: Observed evolution of vertical profiles of stratification and dissolved oxygen in Long Island Sound. *Proc. New England Estuarine Research Society/Long Island Sound Research Conf.*, Groton, CT, Connecticut Sea Grant and New York Sea Grant, 7–12.
- , J. A. Rice, and P. A. Baxley, 2004: Networked acoustic modems for real-time data delivery from distributed moorings in the coastal ocean: Initial system development and performance. *J. Atmos. Oceanic Technol.*, **21**, 331–346.
- Curtin, T. B., J. G. Bellingham, J. Catopovic, and D. Webb, 1993: Autonomous oceanographic sampling networks. *Oceanography*, **6**, 86–94.
- Davis, C. S., S. M. Gallager, M. Marra, and W. K. Stewart, 1996: Rapid visualization of plankton abundance and taxonomic composition using the Video Plankton Recorder. *Deep-Sea Res.*, **43B**, 1947–1970.
- Edwards, C. A., T. A. Fake, and P. S. Bogden, 2004a: Spring-summer frontogenesis at the mouth of Block Island Sound: 1. A numerical investigation into tidal and buoyancy-forced motion. *J. Geophys. Res.*, **109**, C12021, doi:10.1029/2003JC002132.
- , —, Codiga, and P. S. Bogden, 2004b: Spring-summer frontogenesis at the mouth of Block Island Sound: 2. Combining acoustic Doppler current profiler records with a general circulation model to investigate the impact of subtidal forcing. *J. Geophys. Res.*, **109**, C12022, doi:10.1029/2003JC002133.
- Gordon, R. L., 1996: Acoustic Doppler Current Profiler principles of operation: A practical primer. 2d ed. Broadband ADCPs user's guide, RD Instruments, P/N 951-6069-00, 46 pp.
- Kirincich, A., 2003: Structure and variability of a coastal front. M.S. thesis, Graduate School of Oceanography, University of Rhode Island, 124 pp.
- Large, W. G., and S. Pond, 1981: Open ocean momentum flux measurements in moderate to strong winds. *J. Phys. Oceanogr.*, **11**, 324–336.
- Malone, T. C., and M. Cole, 2000: Toward a global scale coastal ocean observing system. *Oceanography*, **13**, 7–11.
- Piasecki, M., L. Bermudez, S. Islam, and F. Sellerhoff, 2003: IM2: A web-based dissemination system for now and forecast data products. *Proc. Eighth Int. Conf. Estuarine and Coastal Modeling*, Monterey, CA, ASCE, 37–54.
- Rice, J. A., R. K. Creber, C. L. Fletcher, P. A. Baxley, K. E. Rogers, and D. C. Davison, 2001: Seaweb undersea acoustic nets. Space and Naval Warfare Systems Center San Diego Tech. Doc. TD 3117, 17 pp.
- Ullman, D. S., and P. C. Cornillon, 1999: Satellite-derived sea surface temperature fronts on the continental shelf off the northeast US coast. *J. Geophys. Res.*, **104**, 23 459–23 478.
- , and D. L. Codiga, 2004: Seasonal variation of a coastal jet in the Long Island Sound outflow region based on HF radar and Doppler current observations. *J. Geophys. Res.*, **109**, C07S06, doi:10.1029/2002JC001660.